Section III

Comparative Study of Rh/Al_2O_3 and $Rh\text{-}Mo/Al_2O_3$ Catalysts

Research Context

In this section we return to the analysis of Rh/Al_2O_3 and $Rh\text{-}Mo/Al_2O_3$ catalysts synthesized via sequential chemisorption of mononuclear organometallic precursors, namely $Rh(CO)_2(acac)$ and $Mo(CO)_6$. The focus of the investigations presented herein also return to the working hypothesis of our global efforts in the Rh-Mo system, i.e. the idea that Mo serves primarily as a textural promoter, site isolating small Rh aggregates. Here, the influence of the Mo is assessed directly through both CO hydrogenation and infrared spectroscopic analysis of the samples after exposure to room temperature and high temperature syngas environments. The comparisons center on testing Mo-promoted and unpromoted Rh catalysts of similar Rh loadings head-to-head and assessing their activity and oxygenate selectivity, as well as comparing the CO-active infrared frequencies of the samples. As discussed below, the microreactor analysis for CO hydrogenation and the insights gained from infrared spectroscopic characterization of the samples are well aligned with the idea that the Mo, indeed, stabilizes small, isolated Rh aggregates. The Mo-promoted samples tend toward higher oxygenate selectivity and enhance the intensity of the Rh "gem-dicarbonyl" infrared band, the primary marker for highly dispersed Rh. Again, Section I of this report explores an alternative synthesis approach to form $Rh\text{-}Mo/Al_2O_3$, and Section II traces the surface features of the catalytic materials during the synthesis process. In the investigations outlined in this section, we turn back to the origin of our interest in this catalytic system: the unique synergy of Rh and Mo for oxygenate synthesis.

The theme common to each proposal is that the rhodium active sites are isolated by molybdenum (oxide) and the site-isolated rhodium acts much like molecular rhodium complexes in homogeneous catalysis. Better understanding of this site-isolation effect is important for the design of new bimetallic catalysts—both rhodium and non-rhodium systems—for oxygenate synthesis from syngas. This work has focused on the comparative study of Rh/Al_2O_3 and $Rh-Mo/Al_2O_3$ catalysts using CO hydrogenation as a probe reaction and *in situ* infrared (IR) spectroscopic characterization of CO-pretreated catalysts.

Experimental

Catalysts preparation employs the method of non-aqueous sequential chemisorption of metal-carbonyl complexes on alumina, which was developed previously [Foley et al., 1990]. The metal-carbonyl precursors and support material are $Mo(CO)_6$, $Rh(CO)_2$**acac**, and gamma alumina (BET surface area = 250 m^2/g), respectively. The catalysts are listed with their elemental analysis data in the following Table:

Table 1. Rh/Al_2O_3 and $Rh-Mo/Al_2O_3$ catalysts

Catalyst	Rh wt.%	Mo wt.%	Rh/Mo (mole ratio)
Rh-I	0.23	0	--
Rh-II	0.45	0	--
Rh-III	1.37	0	--
Rh-IV	2.66	0	--
RhMo-I	0.21	1.40	0.14
RhMo-II	0.41	1.42	0.27
RhMo-III	1.21	1.46	0.77
RhMo-IV	2.43	1.23	1.84

CO hydrogenation reactions were performed in a fixed bed, down-flow, high-pressure microreactor system, which consists of *(i)* high purity CO and H_2 gas sources, which were further purified by series of traps to exclude H_2O, O_2, $Fe(CO)_5$, etc. *(ii)* a stainless steel tubular reactor with capacity of 0.2-2.0g of catalyst, connected to the gas sources through high pressure

mass-flow controllers, *(iii)* a product analysis unit, in which the downstream mixture of reactants and products were sent to on-line GC's after releasing pressure through a back-pressure regulator. More detailed descriptions of the system can be seen elsewhere [Foley et al.,1990].

Each of the catalysts listed above was reduced at 300°C with H_2 for 3 h before introducing the reactant mixture. Reaction conditions are 473-623K, 2.0-6.6MPa, CO/H_2 = 1/1, and GHSV = $3500h^{-1}$. Data comparing activity and selectivity were collected after the steady-state activity had been reached on the catalysts after about 10 h. on stream. In order to assure differential reaction conditions, CO conversions on all the catalysts are maintained below 10% by diluting the catalyst bed with inert, low surface area quartz chip.

In situ IR studies of the catalysts were performed on a Nicolet 510M FT-IR spectrometer using self-supporting sample wafers in an quartz cell equipped with NaCl windows. All spectra were recorded in flowing helium at room temperature after the sample was treated in CO at different conditions. Each spectrum was recorded using 50 scans with resolution of 4 cm^{-1}.

Results and Discussions

1. Activity and selectivity of the catalysts

To examine the effect of different rhodium loadings and different Rh/Mo ratios on catalytic performance, each catalyst was tested for CO hydrogenation under the same reaction conditions. The stability of the catalysts are shown in the Figures 1 and 2.

It can be seen that all the catalysts have reached relatively stable activities after approximately 8-10 h. But differences are apparent between the rhodium and the rhodium-molybdenum systems. Rh/Al_2O_3 catalysts exhibit gradually decreasing activities with increasing reaction time (Figure 1). In contrast, most of the molybdenum-promoted rhodium catalysts show stable or somewhat increased activities during the same reaction period (Figure 2).

Another significant difference is in the activities of the two series of catalysts. Rh-Mo/Al_2O_3 catalysts have approximately 5-fold higher activities compared with corresponding, unpromoted rhodium catalysts (Figure 1 and 2, Table 2). An interesting fact observed from this reaction data is that with the exception of Rh-I (lowest Rh loading in the group), Rh/Al_2O_3 catalysts have similar turnover frequencies (TOF) which may imply that the nature of the active site on these catalysts are the same or similar despite differences in Rh loading. The exception of Rh-I may be because the Rh loading is not high enough to form similar active sites to those in more highly loaded catalysts. For the molybdenum-promoted system, similar behavior is observed but with exception of both high and low rhodium loadings, RhMo-I and RhMo-IV (Figure 2). This may imply that RhMo-II and RhMo-III have similar active sites but the nature of the active sites are very different from that in the corresponding Rh monometallic system. The idea of probing the nature of active sites from TOF has been used extensively for iron catalysts in ammonia synthesis (see, for example, Topsoe et al 1980). For RhMo-IV the low Mo/Rh ratio may not provide enough physical promoter to form the active sites present in RhMo-II and RhMo-III for oxygenate formation, and hence, the inadequately promoted rhodium on RhMo-IV behaves more like a F-T and water gas shift catalyst with enhanced formation of CH_4 and CO_2. (Table 3). The behavior of the RhMo-I catalyst may be due to the low rhodium loading, as in Rh-I.

From the reaction testing, some broad distinctions can be made about these catalysts:

(1) Mo-promotion significantly enhances oxygenate selectivity, as has been shown in previous investigations;

(2) Oxygenate formation may require a minimum ensemble of rhodium sites as evidenced by the poor performance of Rh-I and RhMo-I samples;

(3) Parity in the Rh and Mo concentrations seems to improve the oxygenate selectivity (compare the performance of RhMo-II and RhMo-III to the promoter-lean RhMo-IV).

Table 2. Summary of the reaction data*

	ΣC_1-C_6	ΣOxy	CO conv.	Rate
Rh-I	82.2%	17.8%	0.16%	1.21E-03
RhMo-I	83.0%	17.0%	0.12%	7.31E-03
Rh-II	93.3%	6.7%	1.59%	6.10E-03
RhMo-II	61.8%	38.2%	1.08%	3.32E-02
Rh-III	91.4%	8.6%	4.36%	6.96E-03
RhMo-III	58.8%	41.2%	1.53%	3.19E-02
Rh-IV	91.1%	6.7%	7.28%	7.41E-03
RhMo-IV	64.6%	25.6%	3.69%	3.85E-02

*Reaction condition: 300°C, 300psi, GHSV=3500/h. Rate: mol CO/mol Rh•sec.

Table 3. Product Selectivity (%) (300°C, 300psi, CO/H_2=1/1)

	CO_2	CH_4	C_2H_6	C_3H_8	Me_2O	MeOH	C_4	EtOH	MeOEt	C_5	C_6
Rh-I	0.0	42.6	12.3	7.6	5.3	12.4	19.7	0.0	0.0	0.0	0.0
RhMo-I	0.0	39.4	24.1	14.6	7.8	9.2	4.9	0.0	0.0	0.0	0.0
Rh-II	0.0	69.4	4.6	4.2	1.3	5.4	9.8	0.0	0.0	3.6	1.7
RhMo-II	0.0	44.0	8.2	3.5	8.1	14.0	1.6	9.1	7.0	4.2	0.2
Rh-III	0.0	73.9	3.4	3.3	0.2	1.8	4.5	1.0	5.6	3.1	3.2
RhMo-III	0.0	45.6	7.6	2.2	5.4	20.0	1.1	8.0	7.9	1.1	1.2
Rh-IV	2.2	76.4	3.1	3.6	0.2	1.6	2.9	0.7	4.2	2.6	2.6
RhMo-IV	9.8	48.1	7.6	2.6	2.2	9.4	1.0	4.5	9.4	4.2	1.2

2. Effect of Temperature and Pressure on Selectivity

Generally, activities increases with increasing reaction temperature for both Rh/Al_2O_3 and $Rh\text{-}Mo/Al_2O_3$ catalysts. However, molybdenum promotion can greatly suppress hydrocarbon formation (principally CH_4) and enhance oxygenated product selectivity on rhodium catalysts. Figures 3 and 4 clearly show this difference for Rh-III and RhMo-III catalysts.

Pressure does not appear to strongly influence the selectivity of the reaction in the range of 2.0 MPa to 6.6 MPa. A slight increase in oxygenate selectivity was observed with increasing pressure. Figure 5 presents a representative example for RhMo-III.

3. In situ *IR characterization of the catalysts*

In situ IR studies focused on the characteristic carbonyl absorption of rhodium species, namely, gem-dicarbonyl (2100, 2025 cm^{-1}), terminal carbonyl (2050 cm^{-1}), and bridging carbonyl (~ 1850 cm^{-1}). It has been demonstrated on alumina-supported rhodium catalyst that the formation of gem-dicarbonyl, $Rh(I)(CO)_2$, is an indication of highly dispersed Rh(I) species, and terminal and bridging carbonyls are correlated to the formation of rhodium crystallites. [Yates et al., 1979, Wang and Yates, 1984]. It is also possible that rhodium species are intrinsically highly dispersed on Rh/Al_2O_3 and/or $Rh\text{-}Mo/Al_2O_3$. Comparison of the IR spectra of Rh/Al_2O_3 and $Rh\text{-}Mo/Al_2O_3$ (see below) indicate that the bimetallic catalysts generally show less terminal and bridging carbonyl intensity and more gem-dicarbonyl features than do the unpromoted catalysts. This distinction may imply that rhodium sites on $Rh\text{-}Mo/Al_2O_3$ are intrinsically more isolated.

All the catalyst samples, reduced exactly as in the reaction studies, had been treated by CO at different temperatures followed by *in situ* IR measurement at room temperature in flowing helium. Following room temperature CO-treatment, all samples show gem-dicarbonyl and terminal carbonyl absorption, and higher rhodium-loading catalysts also show bridging carbonyl features.(see spectra of room temperature CO treated samples, spectrum "A" in Figures 6-13)

These predominant gem-dicarbonyl features are expected because it has been concluded that CO treatment of Rh/Al_2O_3 in the presence of surface Al-OH leads to disruption of Rh(0) crystallites and to the formation of isolated Rh(I) sites [Basu et al., 1987, 1988, Van't Blik et al., 1983].

Following higher temperature treatment of the catalysts with CO, gem-dicarbonyl features are enhanced for low Rh-loading catalysts, namely, Rh-I, Rh-II, RhMo-I, RhMo-II (see Figures 6-9). Differences are minimal across these samples except that more terminal carbonyl absorption is seen in the unpromoted samples (Figures 6 and 8). Highly dispersed, gem-dicarbonyls are the predominate species on all the samples with low Rh loadings. In contrast, the difference between the Rh and RhMo series becomes more pronounced for the higher Rh-loading samples following high-temperature CO treatment. (Figures 10-13). Figures 10 and 11 for Rh-III and RhMo-III, respectively, demonstrate that molybdenum promotion stabilizes highly dispersed Rh(I) features. Terminal and bridging carbonyl species became significant on high-temperature, CO-treated Rh-III but not on RhMo-III. Similar rhodium agglomeration has been observed for CO-adsorbed rhodium catalysts at 423 K by Solymosi and Pasztor [Solymosi and Pasztor 1985]. Stabilization of the gem-dicarbonyl features on RhMo-III again suggests stabilization of isolated rhodium aggregates on the alumina surface and a suppression of rhodium agglomeration in the high-temperature CO environment. This difference between RhMo-III and Rh-III correlates with their different activities and selectivities. High-temperature CO treatment of Rh-IV and RhMo-IV promotes strong bridging carbonyl absorption on both samples although somewhat more intense gem-dicarbonyl features remain in RhMo-IV. The enhancement of bridging carbonyl features on RhMo-IV is probably due to the low Mo/Rh ratio, which is suggestive of the lack of sufficient molybdenum to keep rhodium active sites from agglomerating.

Summary

Molybdenum-promoted rhodium catalysts show high activity for CO conversion and much improved selectivity for oxygenates production. *In situ* IR characterization of the corresponding

catalysts reveals that molybdenum effectively hinders rhodium agglomeration. Therefore, molybdenum-promoted, site-isolated rhodium may be responsible for the observed high oxygenate selectivity on Rh-Mo/Al_2O_3 catalysts.

Acknowledgment

Support for this work was provided by the Pittsburgh Energy and Technology Center under auspices of the Department of Energy University Coal Research Program, Grant DE-F622-90PC90291.

References

Basu, P., Panayotov, D., and Yates, Jr., J. T., 1988, Rhodium-Carbon Monoxide Surface Chemistry: The Involvement of Surface Hydroxyl Groups on Al_2O_3 and SiO_2 Supports, J. Am. Chem. Soc., **110**, 2074.

Basu, P., Panayotov, D., Yates, Jr., J. T., 1987, Spectroscopic Evidence for the Involvement of OH Groups in Formation of $Rh^I(CO)_2$ on Metal Oxide Supports, J. Phys. Chem. **91**, 3133.

Foley, H. C., Hong, A. J., Brinen, J. S., Allard, L. F., Garratt-reed, A. J., 1990, Bimetallic Catalysts Comprised of Dissimilar Metals for the Reduction of Carbon Monoxide with Hydrogen. Appl. Catal., **61**,351-375.

Kip, B. J., Hermans, E. G. F., van Wolput, J. H. M. C., Hermans, N. M. A., Van Grondelle, J., and Prins, R., 1987. Hydrogenation of Carbon Monoxide over Rhodium/Silica Catalysts Promoted with Molybdenum Oxide and Thorium Oxide. Appl. Catal., **35**, 109-139.

Solymosi, F., and Pasztor, M., 1985, An Infrared Study of the Influence of CO Chemisorption on the Topology of Supported Rhodium, J. Phys. Chem., **89**, 4789-4793

Sudhakar, C., Bhore, N. A., Bischoff, K. B., Manogue, W. H, and Mills, G. A., 1988, in Ward, J. W. ed. Catalysis 1987, Molybdena Enhanced Rh/Al_2O_3 Catalysts, pp. 115-124. Elsevier Science Publishers B. V., Amsterdam.

Te, M., Lowenthal, E. E., Foley, H. C., 1994, Evidence for Site Isolation in Rh-Mo Bimetallic Catalysts Derived from $CpRhMo(CO)_3(PPh_3)_2$., J. Catal.,**146**, 591-593.

Topsoe, H., Topsoe, N., Bohlbro, H., and Mumesic, J. A., 1980, Supported Iron Catalysts: Particle Size Dependence of Catalytic and Chemisorptive Properties, Proc. 7th Int. Congr. Catal. (Tokyo), Part A, pp. 247-256.

Trunschke, A., Ewald, H., Miessner, H.,Marengo, S., Martinengo, S., Pinna, F., and Zanderighi, 1992, CO Hydrogenation on Mo-promoted Rh/SiO_2 and Rh/ZrO_2 Derived from Metal Carbonyl Clusters, J. Mol. Catal., **74**, 365-377.

Van't Blik, H. F. J., Van Zon, J. B. A. D., Huizinga, T., Vis, J. C, Koningsberger, D. C., Prins, R., 1983, An EXAFS Spectroscopy Study of a Highly dispersed Rh/Al_2O_3 Catalysts: The Influence of CO Chemisorption on the Topology of Rhodium, J. Phys. Chem., **87**, 2264.

Yates, D. J. C., Murrell, L. L., Prestridge, E. B., 1979, Ultra Dispersed Rhodium Rafts: Their Existence and Topology, J. Catal., **57**, 41

List of Figures

Figure 1. Reaction rate as a function of time for Rh/Al_2O_3 catalysts (300°C, 2.0 MPa)

Figure 2. Reaction rate as a function of time for $Rh\text{-}Mo/Al_2O_3$ catalysts (300°C, 2.0 MPa)

Figure 3. Temperature dependence of product selectivity for Rh-III catalyst (2.0 MPa)

Figure 4. Temperature dependence of product selectivity for RhMo-III catalyst (2.0 MPa)

Figure 5. Pressure dependence of product selectivity for RhMo-III catalyst (250°C)

Figure 6. *In situ* IR spectra for Rh-I in He at room temperature after CO treatment at:
A: Room temperature, B: 100°C, C: 200°C.

Figure 7. *In situ* IR spectra for RhMo-I in He at room temperature after CO treatment at:
A: Room temperature, B: 100°C, C: 200°C.

Figure 8. *In situ* IR spectra for Rh-II in He at room temperature after CO treatment at:
A: Room temperature, B: 100°C, C: 200°C.

Figure 9. *In situ* IR spectra for RhMo-II in He at room temperature after CO treatment at:
A: Room temperature, B: 100°C, C: 200°C.

Figure 10. *In situ* IR spectra for Rh-III in He at room temperature after CO treatment at:
A: Room temperature, B: 100°C, C: 200°C.

Figure 11. *In situ* IR spectra for RhMo-III in He at room temperature after CO treatment at:
A: Room temperature, B: 100°C, C: 200°C.

Figure 12. *In situ* IR spectra for Rh-IV in He at room temperature after CO treatment at:
A: Room temperature, B: 100°C, C: 200°C.

Figure 13. *In situ* IR spectra for RhMo-IV in He at room temperature after CO treatment at:
A: Room temperature, B: 100°C, C: 200°C.

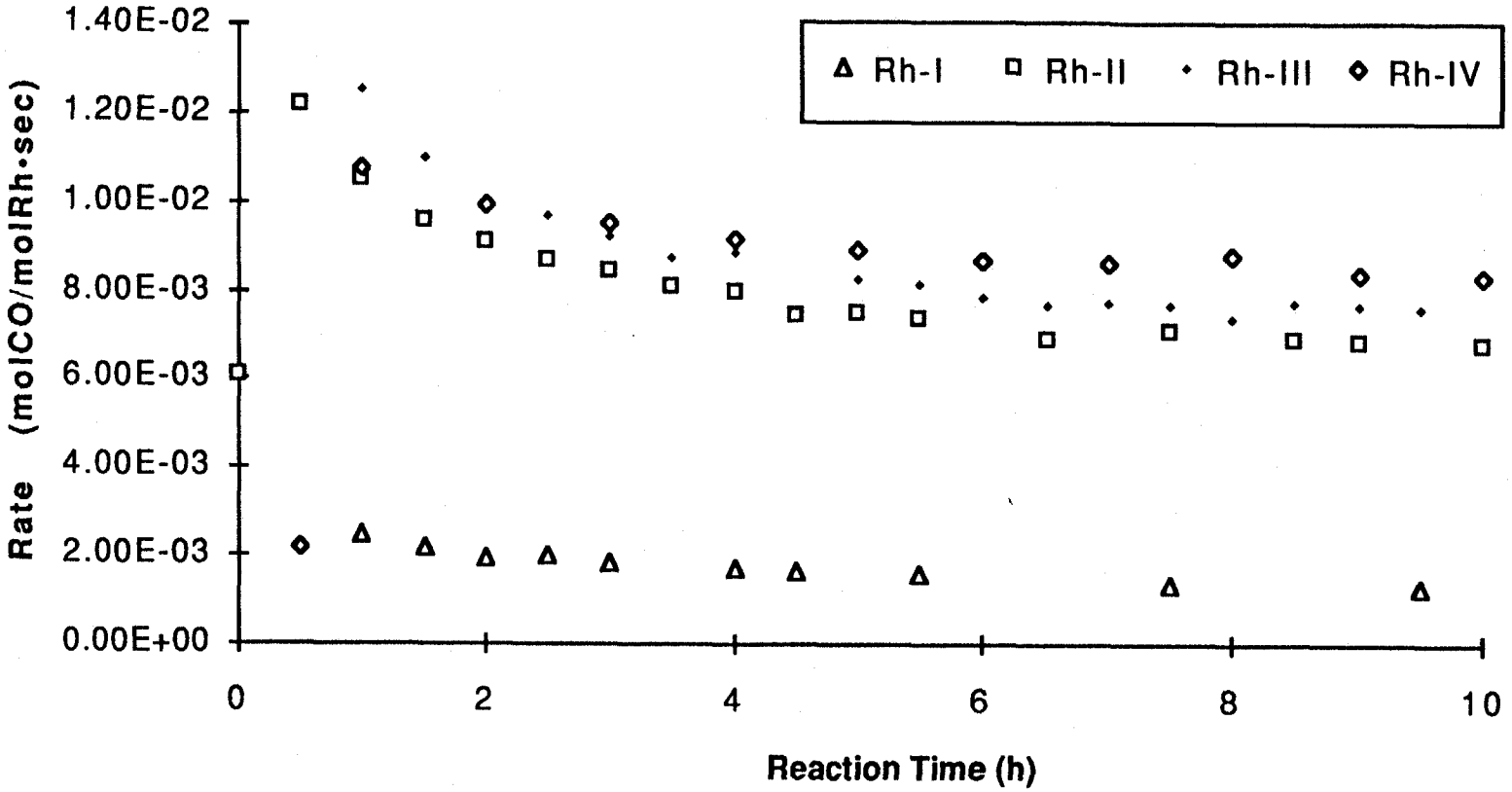
1.40E-02
1.20E-02
1.00E-02
8.00E-03
6.00E-03
4.00E-03
2.00E-03
0.00E+00
Rate (molCO/molRh•sec)
Rh-I
Rh-II
Rh-III
Rh-IV
0
2
4
6
8
10
Reaction Time (h)

Figure 1

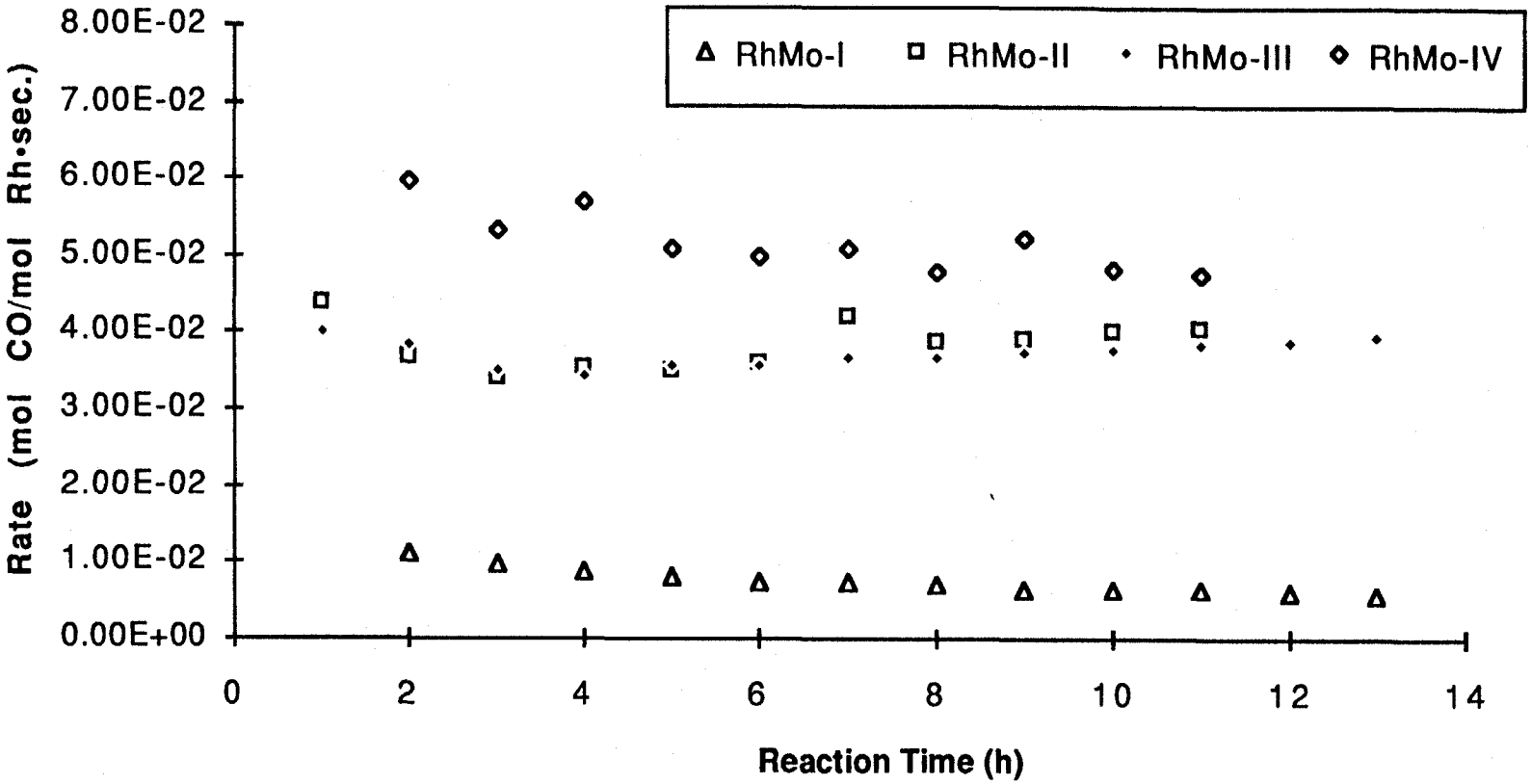
RhMo-I
RhMo-II
RhMo-III
RhMo-IV
Rate (mol CO/mol Rh•sec.)
8.00E-02
7.00E-02
6.00E-02
5.00E-02
4.00E-02
3.00E-02
2.00E-02
1.00E-02
0.00E+00
0
2
4
6
8
10
12
14
Reaction Time (h)

Figure 2

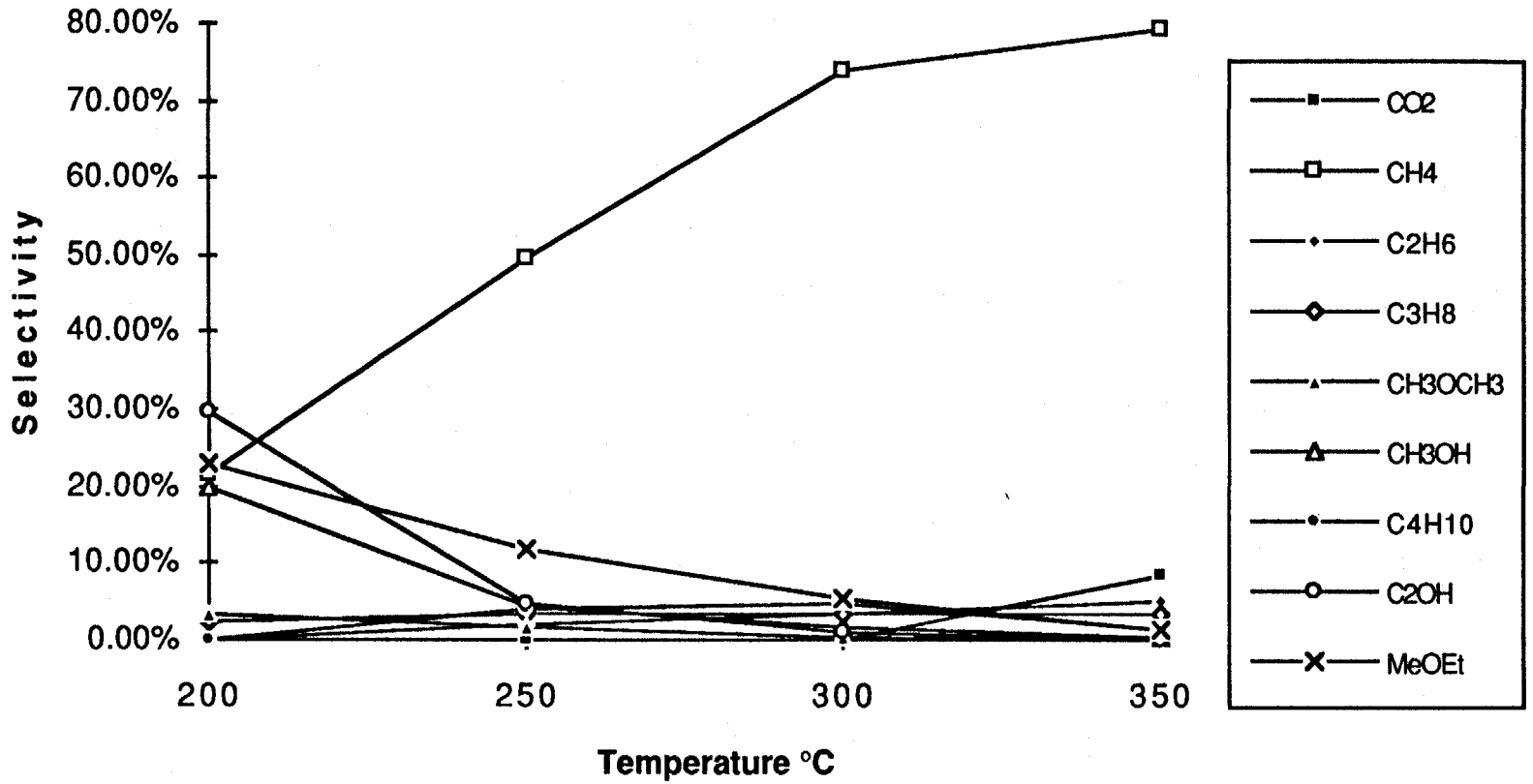
80.00%
70.00%
60.00%
50.00%
40.00%
30.00%
20.00%
10.00%
0.00%
Selectivity
200
250
300
350
Temperature °C
CO2
CH4
C2H6
C3H8
CH3OCH3
CH3OH
C4H10
C2OH
MeOEt

Figure 3

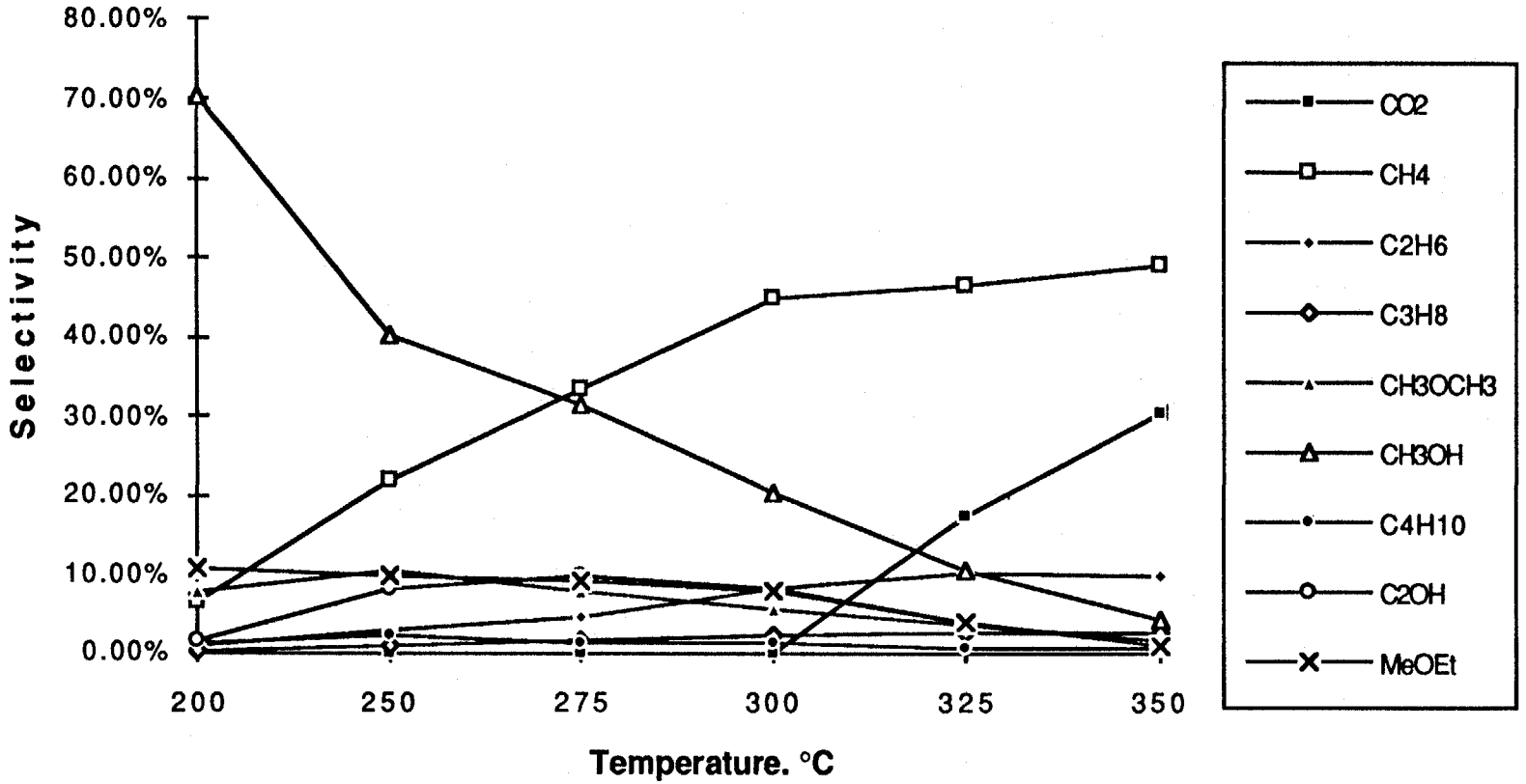
80.00%
70.00%
60.00%
50.00%
40.00%
30.00%
20.00%
10.00%
0.00%
Selectivity
200
250
275
300
325
350
Temperature. °C
CO2
CH4
C2H6
C3H8
CH3OCH3
CH3OH
C4H10
C2OH
MeOEt

Figure 4

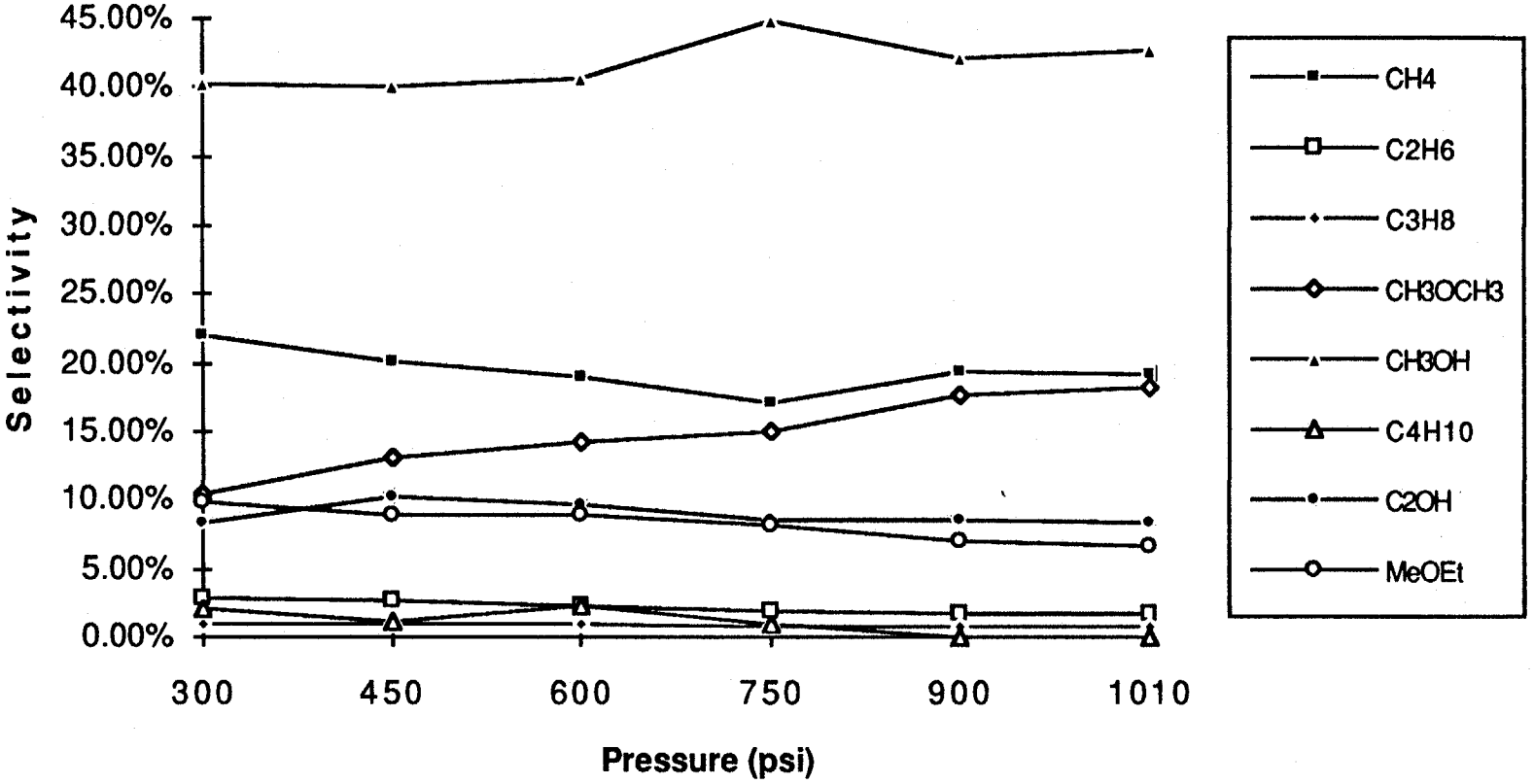
45.00%
40.00%
35.00%
30.00%
25.00%
20.00%
15.00%
10.00%
5.00%
0.00%
Selectivity
300
450
600
750
900
1010
Pressure (psi)
CH4
C2H6
C3H8
CH3OCH3
CH3OH
C4H10
C2OH
MeOEt

Figure 5

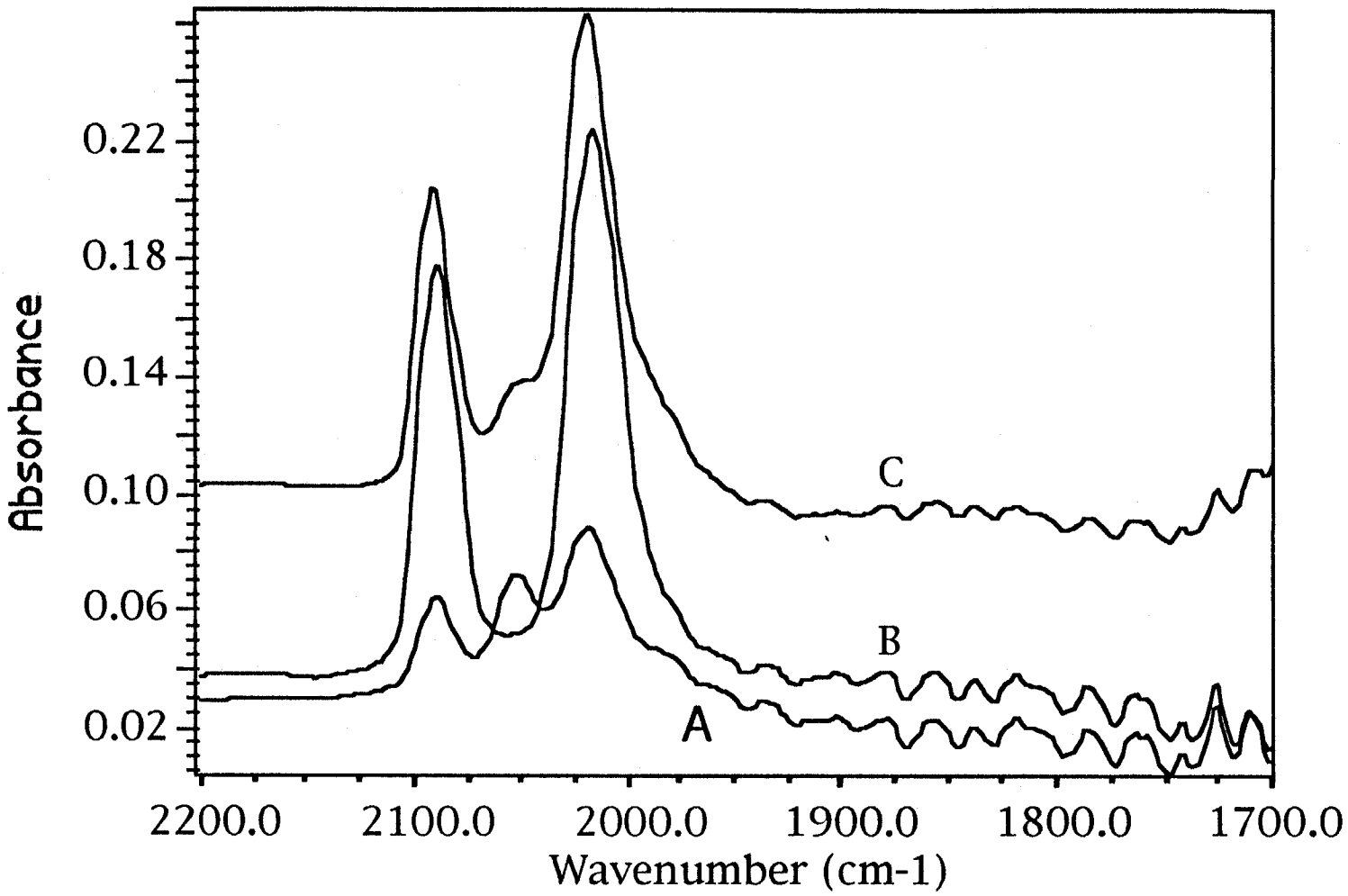
Absorbance
0.22
0.18
0.14
0.10
0.06
0.02
C
B
A
2200.0
2100.0
2000.0
1900.0
1800.0
1700.0
Wavenumber (cm-1)

Figure 6

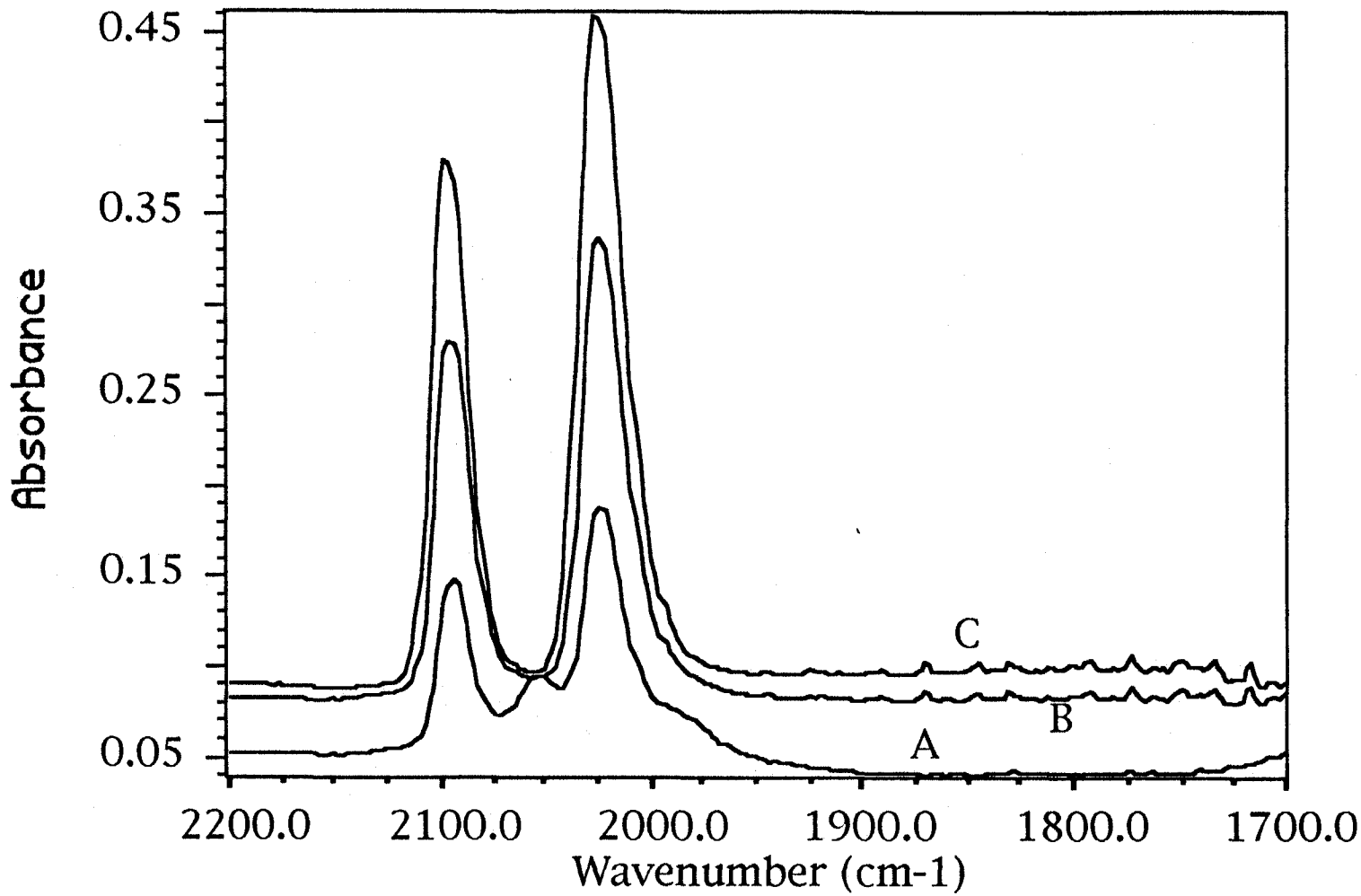
0.45
0.35
0.25
0.15
0.05
Absorbance
C
B
A
2200.0
2100.0
2000.0
1900.0
1800.0
1700.0
Wavenumber (cm-1)

Figure 7

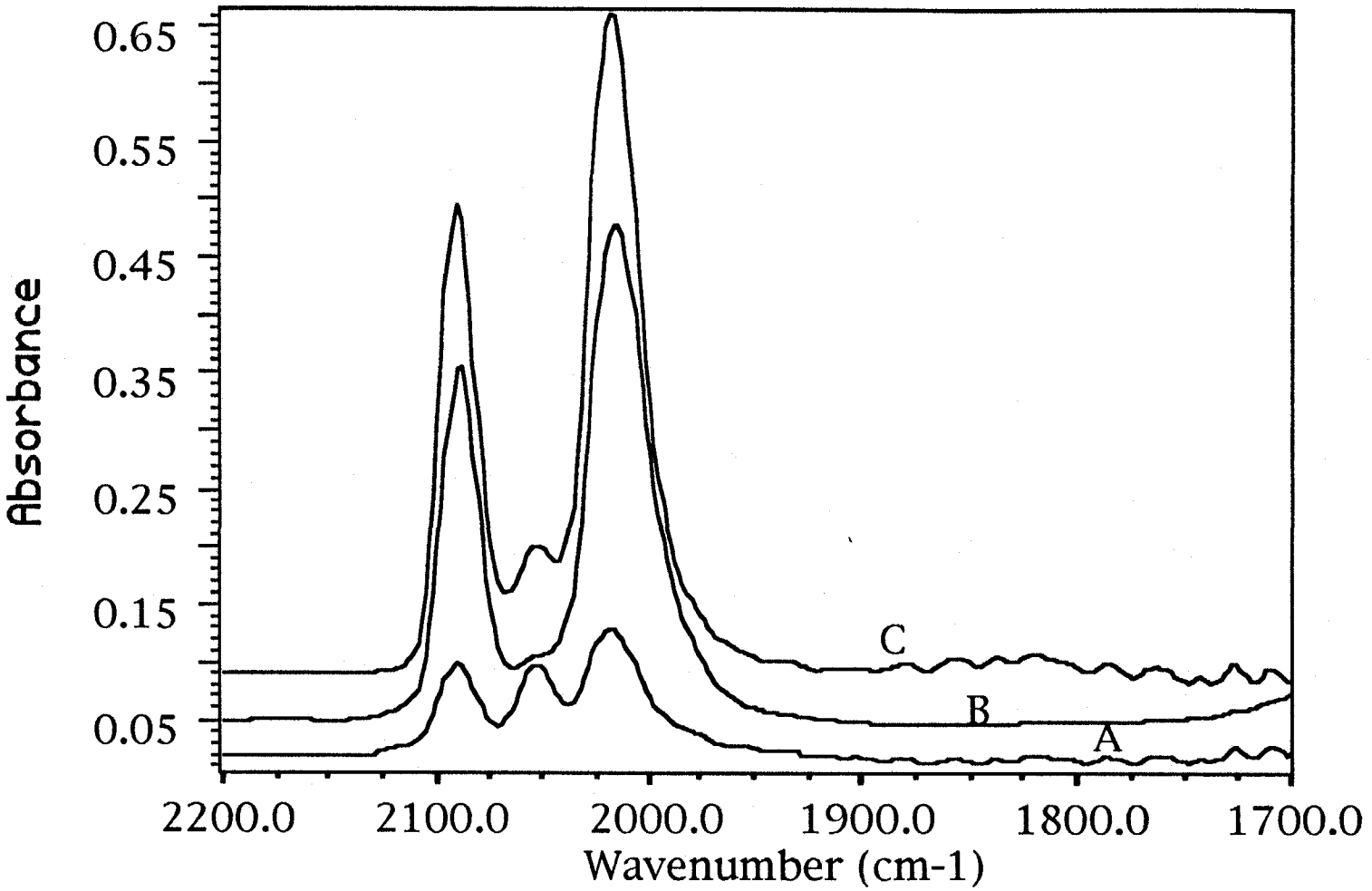
Absorbance
0.65
0.55
0.45
0.35
0.25
0.15
0.05
C
B
A
2200.0
2100.0
2000.0
1900.0
1800.0
1700.0
Wavenumber (cm-1)

Figure 8

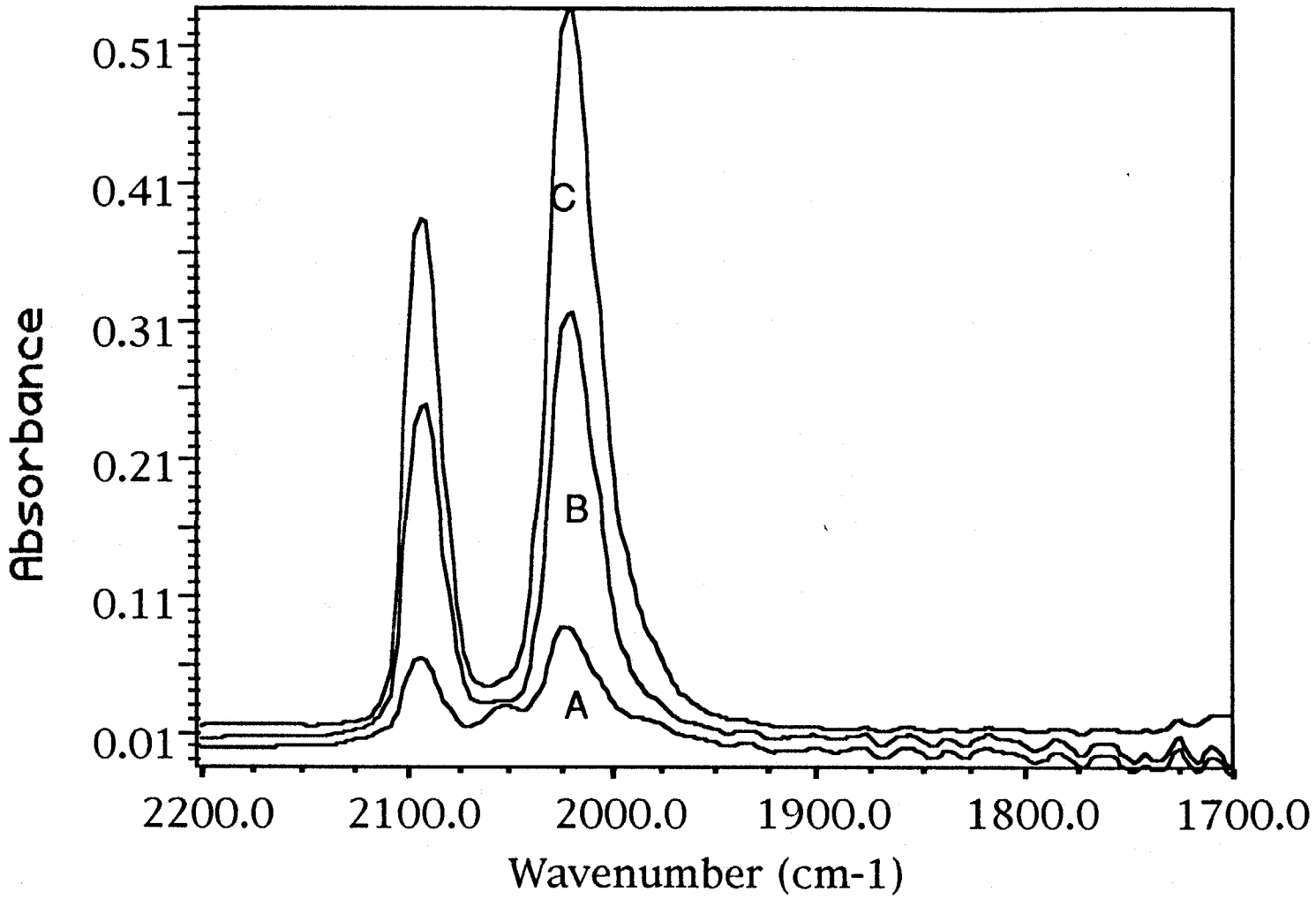
0.51
0.41
0.31
0.21
0.11
0.01
Absorbance
C
B
A
2200.0
2100.0
2000.0
1900.0
1800.0
1700.0
Wavenumber (cm-1)

Figure 9

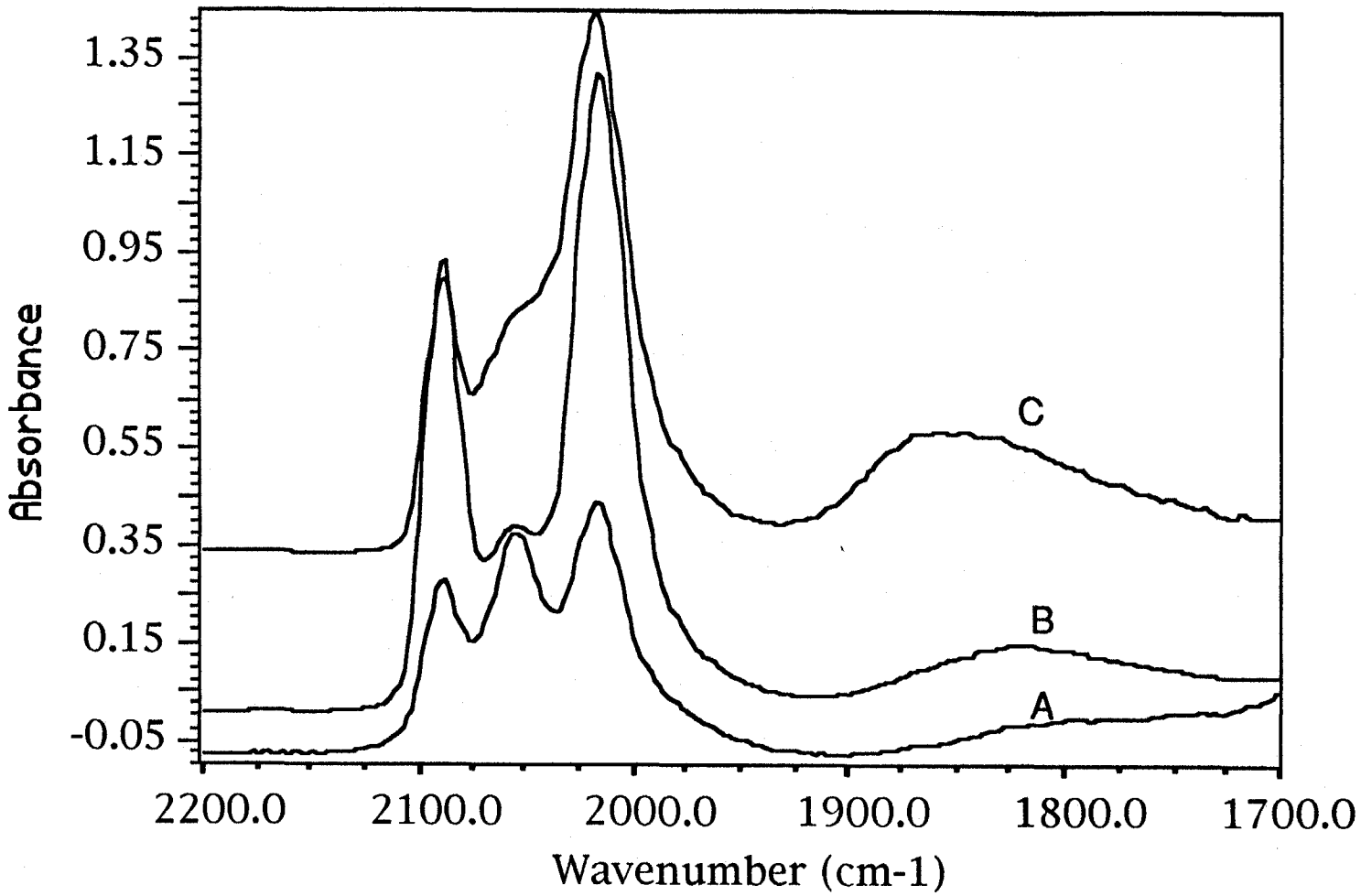
1.35
1.15
0.95
0.75
0.55
0.35
0.15
-0.05
Absorbance
C
B
A
2200.0
2100.0
2000.0
1900.0
1800.0
1700.0
Wavenumber (cm-1)

Figure 10

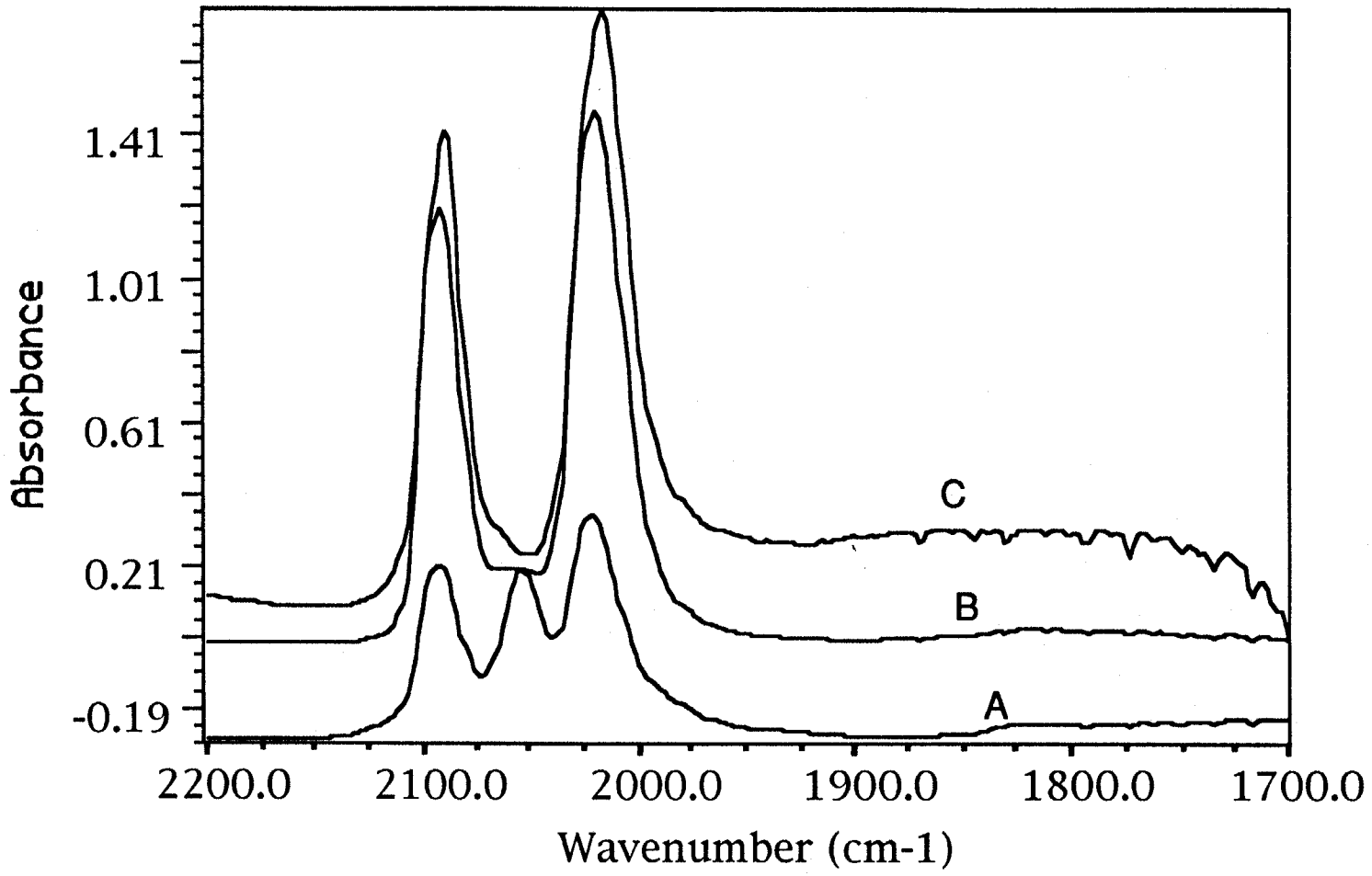
Absorbance
1.41
1.01
0.61
0.21
-0.19
2200.0
2100.0
2000.0
1900.0
1800.0
1700.0
Wavenumber (cm-1)
C
B
A

Figure 11

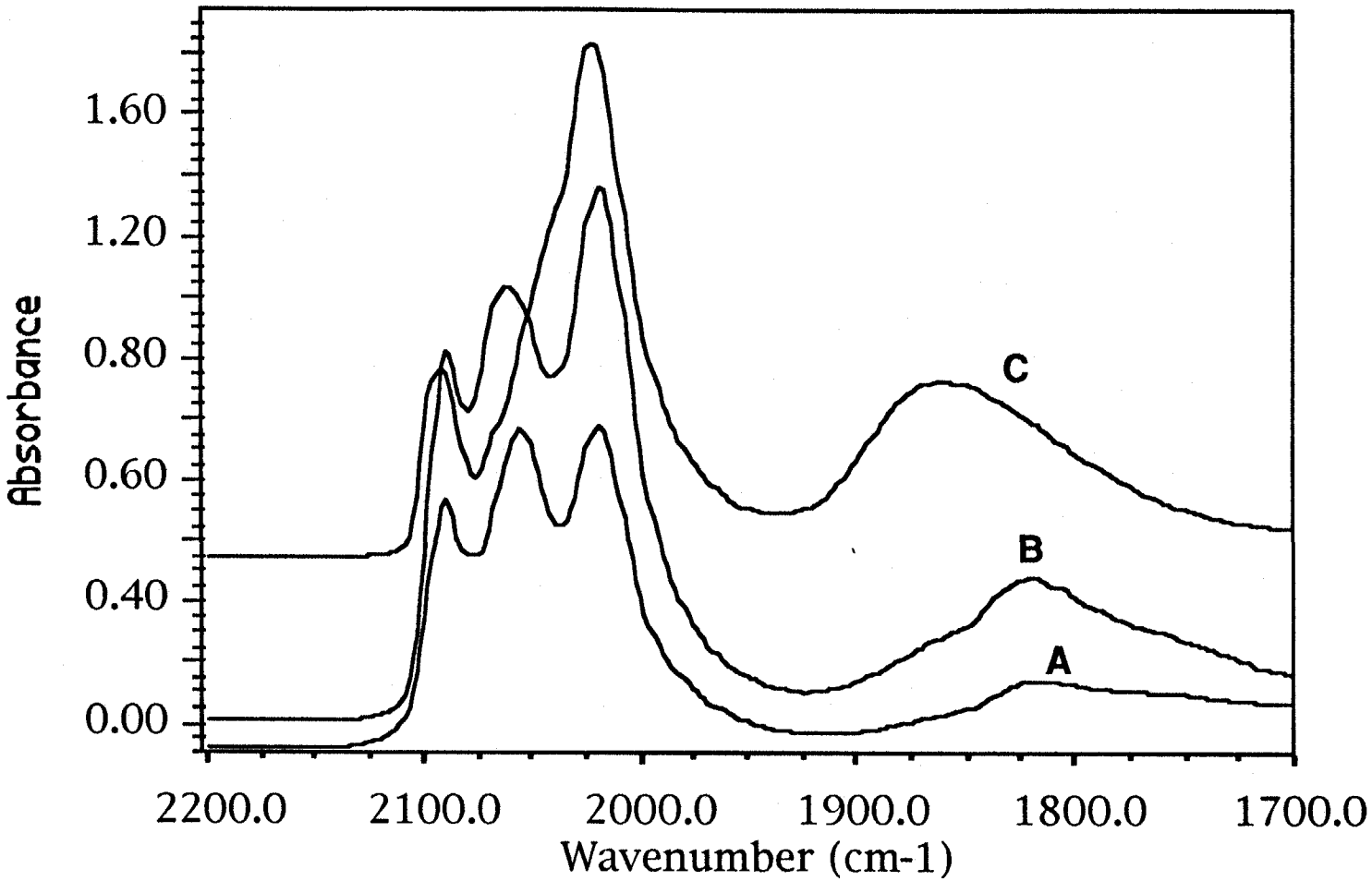
Absorbance
1.60
1.20
0.80
0.60
0.40
0.00
C
B
A
2200.0
2100.0
2000.0
1900.0
1800.0
1700.0
Wavenumber (cm-1)

Figure 12

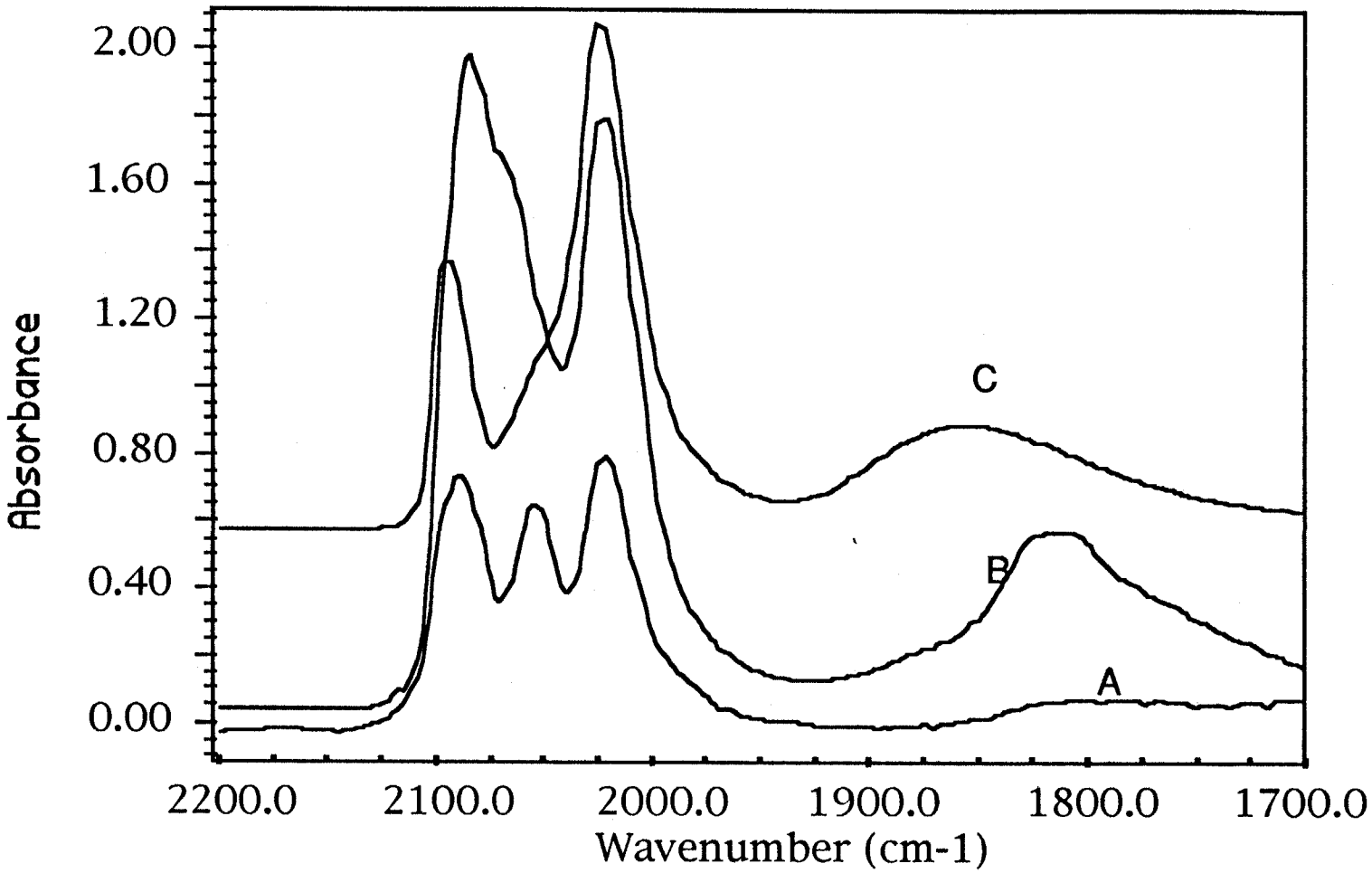
2.00
1.60
1.20
0.80
0.40
0.00
Absorbance
C
B
A
2200.0
2100.0
2000.0
1900.0
1800.0
1700.0
Wavenumber (cm-1)

Figure 13